

Preparation of Activated Carbon Electrode from Pineapple Crown Waste as a Supercapacitor Application 131227

By E. Taer

Preparation of Activated Carbon Electrode from Pineapple Crown Waste as a Supercapacitor Application

E. Taer^{1,*}, A. Apriwandi¹, Y. S. Ningsih¹, R. Taslim², Agustino¹

5

¹ Department of Physics, University of Riau, 28293 Simpang Baru, Riau, Indonesia

² Departement of Industrial Engineering, State Islamic University of Sultan Syarif Kasim, 28293 Simpang Baru, Riau, Indonesia.

*E-mail: erman.taer@lecturer.unri.ac.id

Received: 1 xxx 2019 / Accepted: 1 xxx 2019 / Published: 1 xxx 2019

A pineapple crown activated carbon (PCAC) was prepared from pineapple crown waste using one step carbonisation and physical activation method for electrode super capacitor cells. The pineapple crown waste was also activated by using KOH activation in a ratio of 1 : 1 to the total mass. The pre-carbonised PCAC has a thermal resistance temperature of 300°C while the carbonised one has high Brunauer-Emmett-Teller (BET) with a surface area of 700 m²g⁻¹, a pore volume of 0.362 m³g⁻¹ and an average pore diameter of 22 nm. The surface morphology of pineapple crown electrode shows a good fibre structure with a diameter of 42-73 nm. The electrochemical properties of supercapacitor cells have an excellent specific capacitance which is as high as 150 F g⁻¹ while its energy and power densities are 5.2Wh Kg⁻¹ and 42W Kg⁻¹, respectively

Keywords: pineapple crown; activated carbon; biomass

1. INTRODUCTION

Indonesia is a pineapple producing country whose production reached 1.73 tonnes in 2015 [1]. The waste products derived from this fruit include leaves and crowns. Their crowns are one of the biomass that contains fiber. The size of the fibers can range from nano to micro meters. The shape of its fiber is one of the most developed forms and this is as a result of several advantages such as hollow pores and good electrical conductivity [2]. Ordinary fiber carbon electrodes are produced from materials like polymers which are highly conductive and can be synthesized through chemical processes. Polymer materials that are usually used are pan, pani and other chemicals which are produced at relatively high costs with relatively limited production rates. Biomass material is a natural material with a structure which is more naturally fibrous than that of cellulose fiber. Various types of biomass contain cellulose

fibers that differ in size and amount in percentage and this enables them to produce varying carbon fiber electrodes at relatively low production costs and unlimited quantities. There have been reports of some biomass materials such as banana fiber [3] and oil palm, empty fruit bunches [4], etc which can be used as originating materials for the preparation of carbon fiber electrodes. Carbon fiber has the advantage of being an electrode in an energy storage device such as an electrochemical double layer capacitor that works based on the principle of ion diffusion into the pore of the electrode.

Energy storage occurs because of the presence of layers of ion and electron which are formed in the micro pore of the carbon electrode. The more the ion pairs and electrons which are formed, the greater the amount of energy that can be stored. The formation of ion and electron pairs is affected by the number of micro pores that are available in an electrode. Micro pore electrodes are related to the materials and their activation process. Besides energy, power is the main factor in the performance of EDLC devices. It is related to the speed at which ion is diffused into the pores of the electrode to form ion-electron pairs. This pace is clearly related to the shape of the electrode constituent material and pore size. Over the last decade, the shape of electrode constituent materials has become a fairly extensive study [5]. In this research, a simple method is used to produce carbon fiber electrodes from pineapple crown waste as super capacitor electrodes. Carbon electrodes are provided without additional adhesives they are activated conventionally with focus on the difference in CO₂ activation at temperatures of 600 °C, 700 °C, 800 and 900 °C. The results showed that the optimum activation temperature at which good physical and electrochemical properties of super capacitor cells were produced is 700 °C. The maximum specific capacitance was as high as 150 F g⁻¹ while the dominant carbon fiber had an average diameter size of 68-106 nm.

2. EXPERIMENTAL METHOD

The carbon electrodes of super capacitor from the pineapple crown are produced based on variations in the physical activation temperature. In the first stage, the pineapple crown waste is dried in the sun for 2 days to reduce the moisture content. Pre-carbonization is the process of heating a pineapple crown which is carried out at temperatures ranging from 50°C to 250°C for a period of 2.5 hours. This process always results in fragility and causes carbon to be blackish. Smoothing the pre-carbonized sample is done by using ballmilling and this produces fine pre-carbonized powder [6,7]. This powder is activated chemically using KOH at a ratio of 1:1, then it is converted to monolith form using hydraulic press [8,9]. The next process is the one-step-pyrolysis [10] which is initiated by carbonization at a temperature ranging from 30°C to 600°C under the N₂ gas environment, and followed by physical activation with the temperature constantly being raised to reach the maximum temperature by flowing CO₂ gas for 2.5 hours. The various temperatures for physical activation are 600°C, 700°C, 800°C and 900°C. To facilitate data analysis, the samples were coded as MN600, MN700, MN800 and MN900 for each physical activation temperature variation. Supercapacitor cells are arranged in the form of a sandwich which consists of two carbon electrodes, two current collectors, electrolytes and a separator, such as we have reported in previous studies [11,12]. The electrolytes were made from a solution of H₂SO₄ 1 M [13] while the separator was made from the membrane of duck eggshells [14].

Several characterisations were carried out on pineapple crown carbon electrodes, namely physical and electrochemical characterisations. The physical properties include calculation of density, thermal resistance of biomass materials, crystallinity properties and surface morphology while the electrochemical ones calculated the specific capacitance using the cyclic voltammetry method.

3. DISCUSSION

3.1. Thermal analysis

Figure 1 shows the TGA measurement of pineapple crown powder which has been pre-carbonized at 250°C. The dashed line is a graph of TG in the percentage of the sample mass shrinkage against the temperature. The graph shows three stages of significant sample mass change, the first stage is a decrease in mass with a percentage of 11.99% from room temperature to a temperature of 261.4°C. The process that occurs is the decomposition of water content accompanied by decomposition of complex compounds such as cellulose [15]. The second stage occurs at temperatures ranging from 261.4°C to 318.7°C with a mass loss of 20.3%. This occurrence is the decomposition of hemicellulose, cellulose, and lignin. The decomposition of hemilose mass reaching 55% occurs at between 200°C and 300°C, cellulose mass loss occurs at temperatures ranging from 260°C to 390°C [16]. The rate of lignin is quite slow and it starts from a temperature of 160°C to 900°C. The third stage occurs at temperatures ranging from 318.7°C to 489°C with a mass loss of 21.64%. The total mass lost from these two stages is 41.94%.

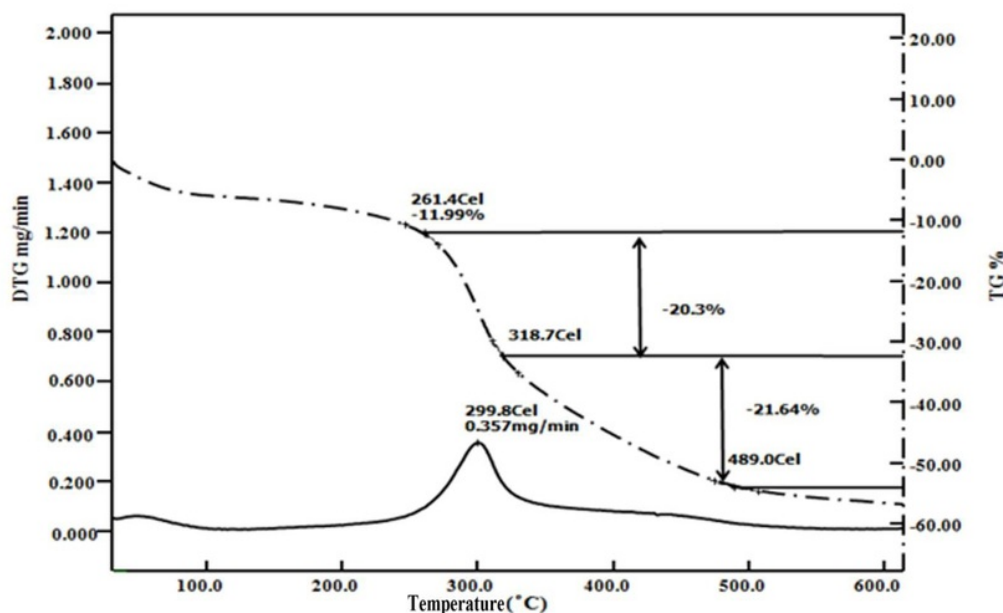


Figure 1. TG and DTG curve for pineapple crown biomass

The remaining sample is carbon material that comes from the pineapple crown. The DTG graph displays the data in form of a straight line that is accompanied by two peaks which determine the maximum mass change rate that occurs in the sample. The decrease in mass from the DTG graph of the time function results in a reduction in weight. The weight loss that occurred in the pineapple crown sample was 0.357mg/min which occurred at a temperature of 299.8°C. At this temperature was select as a thermal resistance in the carbonization process of pineapple crown biomass and hold 1 hour to ensure that this process can occur more perfectly.

3.2. Density analysis

Figure 2 shows the density of each sample. The data shows that the activation temperature affects the density as an increase in the activation temperature from 600°C to 700°C results in a reduction in density. However, the density increases when the activation temperature is increased to 800°C and 900°C. The pyrolysis process causes the carbon condition to be good (non-carbon components have evaporated from the carbon electrodes), resulting in pores on the electrode and decreased density. The carbonization process can remove impure compounds such as water content, oxygen and Nitrogen. This process leaves holes so that the carbon electrode has a large amount of pores. It leaves an imperfect pore structure so that the physical activation process is needed. Physical activation at 700°C produces the lowest density. This is because at this temperature, it is the optimum condition to remove impurities and rearrange the carbon matrix in the electrode. The phenomenon in this study is similar to that in the research conducted by Farma *et al.*, 2015 [17]. In the process of physical activation, a temperature higher than 700°C demonstrates that the release of impurities is more dominant than the rearrangement of the carbon matrix in the electrode sample, this phenomenon is characterised by a smaller electrode mass which causes the sample density to be higher.

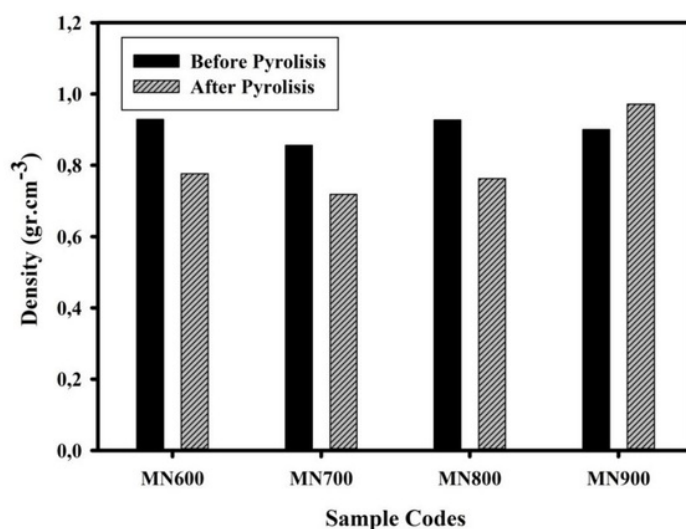


Figure 2. Density of carbon electrode samples

3.3. X-ray Analysis

3 Figure 3 is a graph of the relationship between X-ray intensity to scattering angle (2θ) in pineapple crown carbon samples. The characterisation results show that there are two wide peaks with an angle of 2θ at 24 and 44 which are related to the diffraction plane (002) and (100) [18]. The determination of 2θ angles for each peak was carried out with help from Microcal Origin software. Data is fitted by using the lorentzian distribution function. The results of the fitting obtained data scattering angle, peak height and peak width. These two peaks indicate that the pineapple crown activated carbon electrode is amorphous.

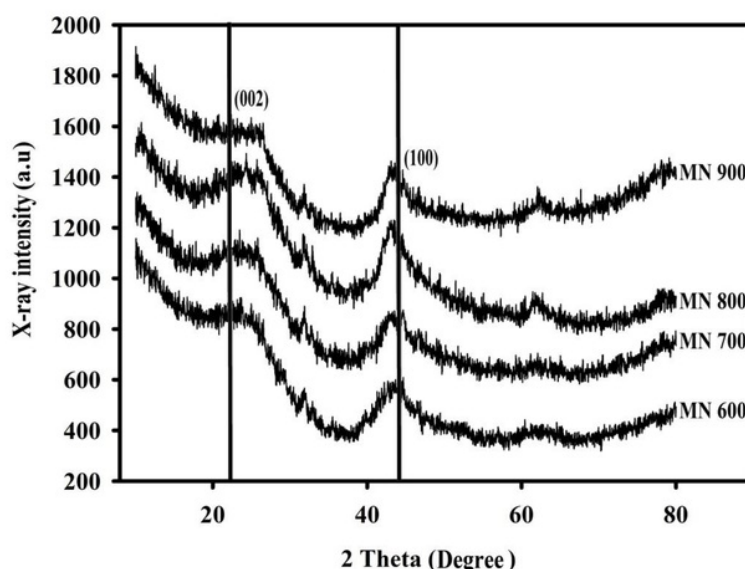


Figure 3. X-ray curve for carbon electrode pineapple crown

Table 1. Data calculation of lattice parameters for monolith pineapple carbon electrodes

Sample codes	$2\theta_{(002)}$ (°)	$2\theta_{(100)}$ (°)	$d_{(002)}$ (Å)	$d_{(100)}$ (Å)	L_c (Å)	L_a (Å)
MN600	24.169	43.986	3.679413	2.056913	12.05188	28.21875
MN700	24.652	44.487	3.608406	2.034904	9.939321	41.65613
MN800	24.564	43.808	3.621134	2.064857	11.50431	44.17795
MN900	24.734	44.001	3.596629	2.056246	11.55130	41.63316

Data calculation of lattice parameters of monolith pineapple carbon electrodes such as peak height (L_c), peak width (L_a) and interlayer spacing (d) are done using the Debye-Scherrer formula [19, 20, 21] and Bragg equation [22], so that the complete data is 2θ , L_c , L_a , and d , as shown in Table 1. It can be seen that the highest L_c is found in the MN600 of 12.05188 Å while the lowest is found in the MN700 sample of 9.939321 Å. The relationship of L_c to surface area is given by the empirical formula

$S=2/\rho_{\text{XRD}}L_c$ with ρ_{XRD} being the XRD density which is obtained from $\rho_{\text{XRD}}=\{d_{002}(\text{graphite})/d_{002}\} \rho(\text{graphite})$ with values of $d_{002}(\text{graphite})=0.33354\text{ nm}$ and $\rho(\text{graphite})=2.268\text{ g cm}^{-3}$ [23,24]. Based on the empirical formula, the X-ray diffraction curve data concluded that the smallest surface area is the MN600 sample while the largest is the MN700 sample.

3.3. Surface morphological analysis

Characteristics of Scanning Electron Microscopy (SEM) aim to determine the surface morphological structure of a material. The result of the characterisation of carbon samples from pineapple crown biomass materials is illustrated in Figures 4 and 5.

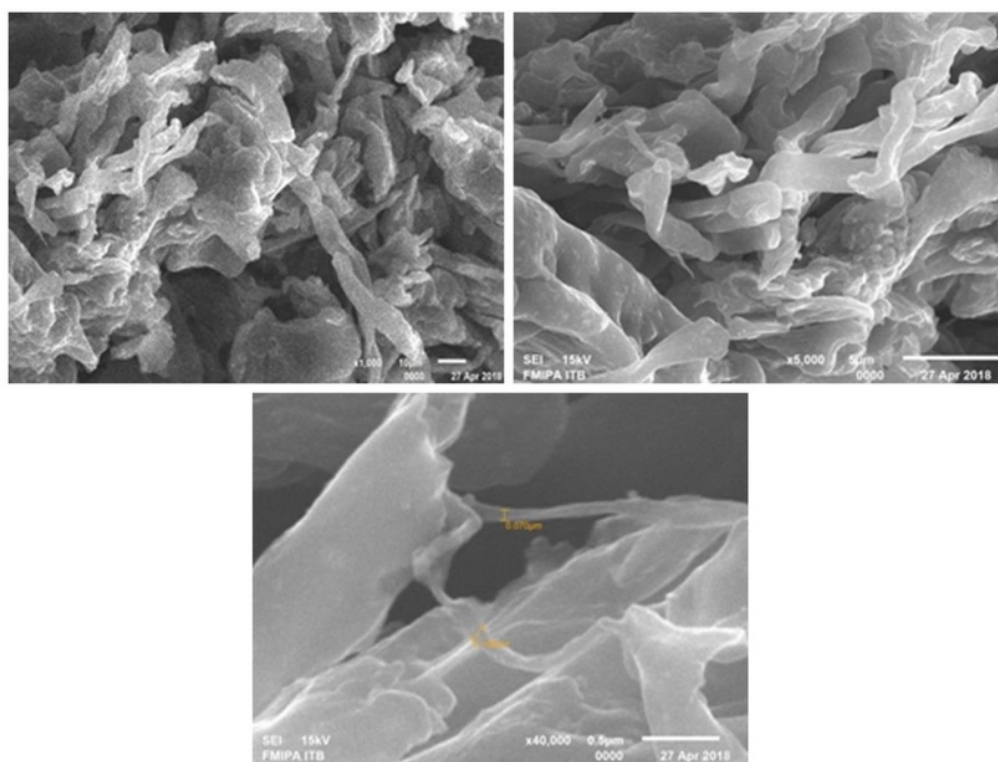


Figure 4. The SEM characterisation for the MN700 sample was carried out using three different magnifications which were a) 1000X; b) 5000X and; c) 40000X

Figures 4 and 5 show the surface morphology of carbon electrode for the MN700 and MN900 samples with three different magnifications of 1000X, 5000X, and 40000X. These Figures demonstrate the fiber contained on the surfaces of the two electrode samples. The presence of carbon fiber comes from cellulose fiber that is naturally present in pineapple crown samples. The MN700 at a magnification of 1000X can be seen in the fiber with a length ranging from $8.643\mu\text{m}$ to $14.080\mu\text{m}$ and

a diameter ranging from $1.019\ \mu\text{m}$ to $1.698\ \mu\text{m}$. At a 5000X magnification, the presence of fiber is clearer, besides that it also shows the presence of pores formed. This can be seen in Figure 4b where there is a dark pattern between visible fibers. Figure 4c is MN700 with a magnification of 40000X which shows a fiber with a length ranging from $0.641\ \mu\text{m}$ to $1.535\ \mu\text{m}$ and a diameter ranging from $0.070\ \mu\text{m}$ to $0.106\ \mu\text{m}$.

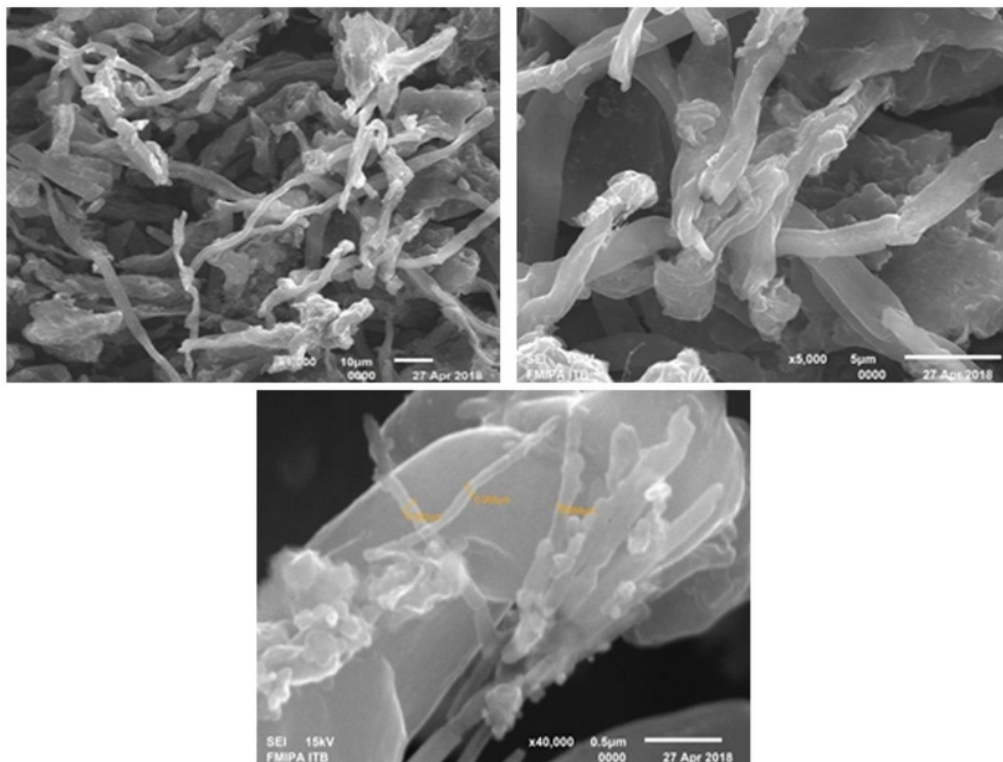


Figure 5. The SEM characterisation for the MN900 sample was carried out using three different magnifications which were a) 1000X; b) 5000X and; c) 40000X

Whereas for the MN900 sample, the presence of carbon fiber appears to be more than that of the MN700. At a magnification of 1000X, the MN900 contained fiber with a length ranging from $21.45\ \mu\text{m}$ to $24.90\ \mu\text{m}$ and a diameter ranging from $0.86\ \mu\text{m}$ to $1.84\ \mu\text{m}$. At a magnification of 5000X, the MN900 fiber is also seen more clearly and at a magnification of 40,000X the fiber length ranged from $0.875\ \mu\text{m}$ to $1.28\ \mu\text{m}$ and the diameters ranged from $0.068\ \mu\text{m}$ to $0.092\ \mu\text{m}$. This length and diameter range is far greater than that of the carbon fiber in the MN700 sample. This is due to the addition of the physical activation temperature caused by the content of non-carbon being released more and causing clumps between fibers to be released and finally the fiber looks more with finer diameter sizes. In a study similar to other biomass materials which had nanofiber such as banana stems [25] and mission grass flower [26] with a fiber sizes ranging from $0.042\ \mu\text{m}$ to $0.131\ \mu\text{m}$ and from $0.042\ \mu\text{m}$ to $0.073\ \mu\text{m}$ respectively.

3.4. EDX analysis

The EDX results for pineapple crown carbon electrode samples obtained the elements of Carbon (C), Oxygen (O), Magnesium (Mg), Silicon (Si), and Calcium (Ca). The elemental and atomic content is expressed in percentage and shown in Table 2. The Table shows that higher physical activation temperatures result in a higher purity of carbon in the pineapple carbon crown. The MN700 and MN900 samples have carbon elements that are as high as 89.21% and 93.63%. The resulting carbon content data are similar to that of other studies on bamboo waste [27], banana stem waste [28] and sago waste [29]. The higher the carbon content in a material, the higher the tendency for a good specific capacitance. The MN900 sample has a higher carbon element than the MN700 sample, but the MN900 has a lower specific capacitance than the MN700. This is due to the fact that a high physical activation temperature would eradicate more impurities in the carbon electrode. A lot of impurities are eradicated, resulting in particles getting denser which causes the flow of ions in the pore to be blocked so that the specific capacitance obtained decreases. This analysis is supported by high MN900 electrode density compared to MN700 electrode density. From Table 2, it can be seen that activated carbon electrode also contains other elements besides carbon, such as oxygen. This is because of the oxygen content left due to incomplete carbonization or bonding which can also occur in the activation process [30]. The weight percentage and the atomic percentage of the MN700 sample are higher than those of the MN900, the percentages are 7.89% and 6.15% for the MN700 sample while for the MN900, they are 6.78% and 5.26%. There are also other elements such as Magnesium (Mg), Silicon (Si) and Calcium (Ca) in the lower percentage.

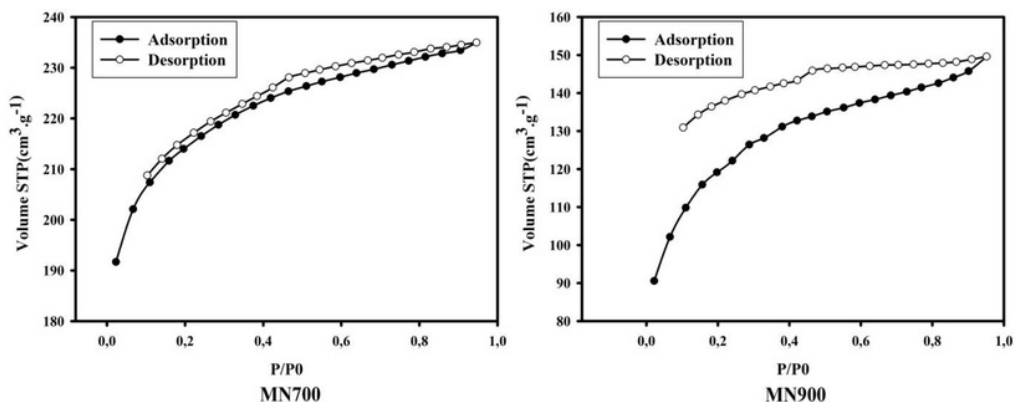
Table 2. The element contents for MN700 and MN900 samples

Component	MN700		MN900	
	Weight %	Atom %	Weight %	Atom %
Carbon	89.21	92.63	90.65	93.63
Oxygen	7.89	6.15	6.78	5.26
Magnesium	1.34	0.69	1.42	0.73
Silicon	0.32	0.14	0.29	0.13
Calcium	1.24	0.39	0.86	0.27

3.5. Surface area analysis

Analysis of N₂ gas absorption was carried out at a temperature of 77.350K which gave an isothermal curve between the relative pressure (P/P₀) to the STP volume (cm³ g⁻¹) and this can be seen in Figure 6. The N₂ gas adsorption process occurs at a relative pressure of 0 - 1 then continues with desorption until it reaches a relative pressure of 0 again. Figure 5 shows that the IUPAC curve formed is the isotherm type II curve [31]. Absorption occurs in mixtures of micropore and mesoporous. Figure 6 shows the amount of gas absorbed by the pineapple carbon related to the relative pressure (P/P₀). The pressure is relatively very influential on N₂ gas uptake which enters the pores of the carbon electrode. Figure 6 shows the relationship of absorption volume to changes in N₂ gas pressure. In the MN700 and

MN900 curves it is shown that the shape of the hysteresis is in the pressure region of 0.1 to 0.9. The MN900 image shows that the hysteresis curve is not completely formed. It is possible that at a temperature of 900°C, the pore structure of the carbon produced is damaged and as a result of this, the resulting curve is not so good. At the relatively low P/P₀ ratio, the formation of micro pores occurs in the carbon sample, then increasing the relative pressure indicates the formation of pores that are larger in the matrix carbon sample [32].



58
Figure 6. Nitrogen adsorption-desorption isotherms for a) MN700; b) MN900

11
The Table 3 shows BET surface area (S_{BET}), BJH surface area (S_{BJH}), BET volume (V_{BET}), BJH volume (V_{BJH}), BJH diameter (D_{BJH}) and average pore diameter (D_{average}). It also shows the surface area of the sample.

11
Table 3. BET surface area (S_{BET}), BJH surface area (S_{BJH}), BET volume (V_{BET}), BJH volume (V_{BJH}), BJH diameter (D_{BJH}) and average pore diameter (D_{average}) of carbon electrodes using BET characterization

Sample codes	S_{BET} (m^2g^{-1})	S_{BJH} (m^2g^{-1})	V_{BET} (m^3g^{-1})	V_{BJH} (m^3g^{-1})	D_{BJH} (Å)	D_{average} (Å)
MN700	684.035	23.854	0.364	0.0278	35.744	21.308
MN900	39.388	16.866	0.231	0.0189	35.590	23.350

The surface area of the sample tends to decrease with increasing activation temperature. In the table there is also other information like the volume of Barrier Joinet Halenda (V_{BJH}). BJH is a method of measuring the pore structure of activated carbon for micropore and mesoporous sizes [33]. Mesopori is related to power while micropore is related to the energy value of super capacitors [34]. The pore volume for the MN700 sample is 0.364 (m^3g^{-1}) and that for the MN900 sample is 0.231 (m^3g^{-1}). The average pore diameter of the sample for the MN700 code is 21.308 nm while that of the MN900 sample

23.350nm. According to the IUPAC classification [31], pores are divided into 3 types, namely micropore ($d < 2\text{nm}$), mesoporous ($2 < d < 50\text{nm}$), and macropore ($d > 50\text{nm}$). Based on this classification, the pineapple crown carbon electrode sample is dominated by mesopores. Table 4 shows the comparison of the surface areas of different biomasses.

Table 4. Comparison of BET surface areas from different biomasses

Biomass	$S_{\text{BET}} (\text{m}^2\text{g}^{-1})$	References
Olive residues	771-1390	35
Cattail	441.12	36
Durian shell	467-979	37
Orange peels	300-620	38
Waste tea	1125-1327	39
Coconut shell	1057	40
Pineapple crown	39-700	Present study

3.6. Electrochemical analysis

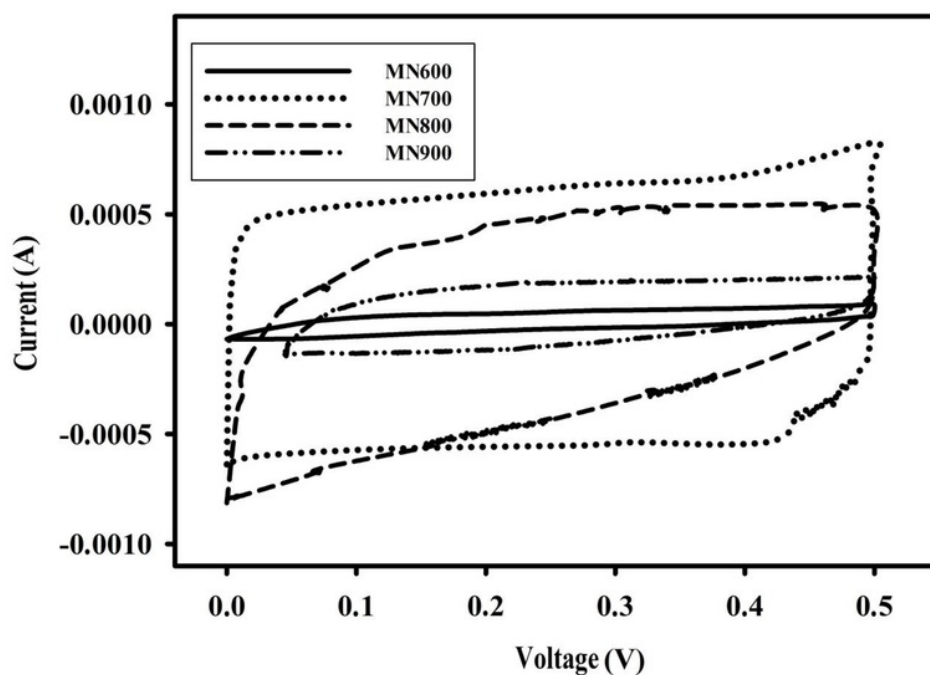


Figure 7. CV curve for all super capacitor cells

Figure 7 is a cyclic voltammogram data that shows the relationship between current and voltage. The charge current (I_c) is shown on the curve from voltage 0 to 0.5 V, while the discharge current (I_d)

is shown at a voltage of 0.5V to 0. Figure 7 shows the width of the I_c and I_d regions. The MN700 cell displays the widest width of the (I_c - I_d) area, followed by the MN800, MN900, and MN600 cells respectively. The I_c and I_d regions are related to the specific capacitance of the supercapacitor cells [41]. It can be observed that the sequence of specific capacitances from the highest to the lowest in relation to electrode samples are MN700, MN800, MN900, and MN600.

Table 5. Specific capacitances of pineapple crown activated carbon electrodes

Sample codes	Mass (g)	I_c (A)	I_d (A)	Specific capacitance (F/g)
MN600	0.00570	0.000052	-0.000015	12
MN700	0.00915	0.000811	-0.000558	150
MN800	0.01115	0.000295	-0.000436	65
MN900	0.00840	0.000188	-0.000099	34

This analysis is in accordance with the specific capacitance data that was obtained using standard formula [42,43] and is completely shown in Table 5. The data presented in Table 5 shows that the MN700 sample has the highest specific capacitance which is as high as 150 F g^{-1} while the MN600 sample shows the lowest which is as high as 12 F g^{-1} . Generally, it can be seen that the increase in activation temperature from 600°C to 700°C results in an increase in the specific capacitance of supercapacitor cell, whereas from 700°C to 900°C , the specific capacitance decreases. 700°C was chosen as the optimum activation temperature, this temperature produced a high pore surface area so that more electrons are trapped inside the pores of the carbon electrode. The maximum capacitance produced in this study is almost the same as the specific capacitance with different biomass materials such as a mixture of rice husk, beet sugar [44] and coffee shell [45] with each of the specific capacitances 116 F g^{-1} and 156 F g^{-1} .

In addition to specific capacitance, the electrochemical properties of supercapacitors can also be analysed by energy and power densities calculated by standard equations [46-47]. The maximum energy and power densities in this study are 5.2 Wh Kg^{-1} and 42 W Kg^{-1} respectively. These are almost the same as other supercapacitors with different biomass materials such as olive residues [35], tobacco waste [48] and bamboo [49].

4. CONCLUSION

As a renewable material, the pineapple crown waste successfully fabricated a pineapple crown activated carbon (PCAC) using one step carbonization and physical activation by N_2 and CO_2 gas. The carbon electrode demonstrated good physical properties such as low density, high carbon content and high surface area. Electrochemical cells of electrode from PCAC showed excellent specific capacitance with high energy and power densities. The reported good physical properties and excellent electrochemical performance promises to transform pineapple crown into a good material for the preparation of activated carbon electrode for super capacitor cell.

ACKNOWLEDGEMENTS

The author would like to thank the DRPM Kemenristek-Dikti through the second year Project of PDUPT with the title "Potential of Urban Solid Waste Utilization as a Supercapacitor Electrode" with contract number: 360/UN.19.5.1.3/PP/2018. The author also thanks the SEM FMIPA ITB Laboratory, which has assisted in obtaining the SEM and EDX data.

References

1. E. Respati, *Pusat Data dan Sistem Informasi Pertanian Sekretariat Jenderal Kementerian Pertanian*, (2016) Jakarta, Indonesia.
2. Yin, Y. Chen, D. Li, X. Zhao, B. Hou, B. Cao, *Material Design*, **111** (2016) 44.
3. K. Chaitra, R.T. Vinny, P. Sivaraman, N. Reddy, K. Venkatesh, C. S. Vivek, N. Nagaraju, K. Athyayini, *J. Energy Chem.*, (2016).
4. M. Deraman, S. K. M. Saad, M. M. Ishak, Awitdrus, E. Taer, I. Talib, R. Omar, M. H. H. Jumali, *the third nanoscale and nanotechnology symposium* (2014) Malaysia.
5. A. Borenstein, O. Hanna, R. Attias, S. Luski, T. Brousse, D. Aurbach, *J. Mater. Chem.*, **5** (2017) 12653.
6. N. S. M. Nor, M. Deraman, R. Omar, E. Taer, Awitdrus, R. Farma, N. H. Basri, B. N. M. Dola, *AIP Conf. Proc.*, 1586 (2014) 68.
7. Taer, M. Deraman, I. A. Talib, S. A. Hashmi, A. A. Umar, *Electrochem. Acta*, **56** (2011) 10217.
8. E. Taer, P. Dewi, Sugianto, R. Syech, R. Taslim, Salomo, Y. Susanti, A. Purnama, Apriwandi, Agustino, R. N. Setiadi, *AIP Conf. Proc.*, 1927 (2018) 030026-1.
9. E. Taer, B. Kurniasih, F. P. Sari, Zulkifli, R. Taslim, Sugianto, A. Purnama, Apriwandi, Y. Susanti, *AIP Conf. Proc.*, 1927 (2018) 030006-1.
10. E. Taer, Apriwandi, Yusriwandi, W. S. Mustika, Zulkifli, R. Taslim, Sugianto, B. Kurniasih, Agustino, P. Dewi, *AIP Conf. Proc.* 1927 (2018) 030036-1.
11. Deraman, R. Omar, S. J. Zakaria, *J. Mater. Sci.*, **7** (2002) 3329.
12. R. Farma, M. Deraman, A. Awitdrus, I. A. Talib, E. Taer, J. G. Manjunatha, M. M. Ishak, B. N. M. Dollah, S. A. Hashmi, N. H. Basri, *Bioresour. Technology*, **132** (2013) 254.
13. Iwantonono, E. Taer, A. A. Umar, *AIP Conf. Proc.*, 1454 (2012) 251.
14. E. Taer, Sugianto, M. A. Sumantre, R. Taslim, Iwantonono, D. Dahlan, M. Deraman, *Adv. Mater. Research*, 896 (2014) 66.
15. L. L. Zhang, S. X. Zhao, *Chemical Society Reviews*, **38** (2009) 2520.
16. Brebu, C. Vasile, *Cellulose Chemistry Technology*, **49** (2010) 353.
17. R. Farma, M. Deraman, Awitdrus, I. A. Talib, R. Omar, J. G. Manjunatha, M. M. Ishak, N. H. Basri, N. M. Dollah, *Int. J. Electrochem. Sci.*, **8** (2013) 257.
18. G. Yu, L. Lei, J. Yuming, W. Yu, Y. Chuanjun, W. Yingjin, C. Gang, G. Junjie, L. Haiyan, *Appl. Energy*, **153** (2015) 41.
19. D. Cullity, *Elements of X-Ray Diffraction*, Ed. 3, (2001) Amazon Prentice Hall.
20. M. V. Nabais, J. G. Teixeira, I. Almeida, *Bioresour. Technol.*, **102** (2010) 2781.
21. Awitdrus, M. Deraman, I. A. Talib, R. Omar, M. H. Jumali, E. Taer, M. H. Saman, *Sains Malaysiana*, **39** (2010) 83.
22. A. González, E. Goikolea, J. A. Barrena, R. Mysyk, *Renewable and Sustainable Energy Reviews*, **33** (2016) 1189.
23. K. Kumar, R. K. Saxena, R. D. Kothari, K. Suri, N. K. Kaushik, J. N. Bohra, *Carbon*, **35** (1997) 1342.
24. M. Deraman, R. Daik, S. Soltaninejad, N. S. M. Nor, Awitdrus, R. Farma, N. F. Mamat, N. H. Basri, M. A. R. Othman, *Adv. Materials Research*, **1108** (2015) 1.

25. E.Taer, R. Taslim, W.S. Mustika, B. Kurniasih, Agustino, A. Afrianda, Apriwandi, *Int. J. Electrochem. Sci.*, 13 (2018) 8428.
26. Zulki³⁴ Awitdrus, E. Taer, *J. Aceh Phys. Soc.*, 7, (2018) 30.
27. ² Z. Zhang, Z. J. Xing, Z. K. Duan, M. Li, Y. Wang, *Applied Surface Science*, 315 (2014) 279.
28. E. Taer, Y. Susanti, Awitdrus, Sugianto, R. Taslim, R. N. Setiadi, S. Bahri, Agustino, P. Dewi, B. Kurniasih, *AIP Conf. Proc.*, 1927 (2018) 030016-1.
29. E. Taer, A. Afrianda, Apriwandi, R. Taslim, A. Agustino, Awitdrus, and R. Farma, *Int. J. Electrochem. Sci.*, 13 (2018) 10688.
30. ¹⁶ Jankowski, A. Swiatkowski, J. Choma, Active Carbon, Ellis Horwood, (1991) London.
31. W. S. K. Sing, H. D. Everett, W. A. R. Haul, L. Moscou, A. R. Pierotti, J. Rouquerol, T. ¹⁵ mieniewska, *Pure & App. Chem.*, 57 (1985) 603.
32. W. R. Li, D. H. Chen, Z. Li, Y. F. Shi, Y. Wan, G. Wang, Z. Y. Jiang, D. Y. Zhao, *Carbon*, 45 ¹⁴ (07) 1757.
33. X. Wu, X. Hong, Z. Luo, K.S. Hui, H. Chen, J. Wu, K.N. Hui, L. Li, J. Nan, Q. Zhang, *Electrochem. Acta*, 89 (2013) 400.
34. ²⁷ S. Huang, B. G. Sumpter, V. Meunier, *Angewandte Chemie International Ed* 47 (2008) 520.
35. A. Elmouwahidi, E. Bailon-Garcia, A. F. Perez-Cadenas, F. J. Maldonado-Hodar, F. Carrasco-⁵⁷ rin, *Electrochem. Acta* 229 ⁶⁴ 17) 219.
- ³⁰ M. Yu, Y. Han, J. Li, L. Wang, *Chemical Engineering Journal*, 317 (2017) 493.
37. T. C. Chandra, M. M. Mirna, J. Sunarso, Y. Sudaryanto, S. Ismadji, *J. Taiwan Institute of Chemical ²⁶ Engineers*, 40 (2009) 457.
38. M. E. Fernandez, B. Ledesma, S. Román, P. R. Bonelli, A. L. Cukierman, *Bioresource Technology*, ²⁴ 3 (2015) 221.
39. I. I. G. Inal, S. M. Holmes, A. Banford, Z. Ak³⁸, *Applied Surface Science*, 357 (2015) 696.
40. J. Katesa, S. Junpirom, C. Tangsathitkulchai, *TIChE International Conference 2011*, November 10 – ⁶ 2011 at Hatyai, Songkhla Thailand.
41. E. J. Ra, E. Raymundo-Piñero, Y. H. Lee, F. Béguin, *Carbon*, 47 (2009) 84.
42. L. Li, E. Liu, J. Li, Y. Yang, H. Shen, Z. Huang, X. Xiang, W. Li, *Journal of Power Sources*, 195 ¹⁷ (2010) 1516.
43. L. Q. Mai, A. Minhas-Khan, X. C. Tian, K. M. Hercule, Y. L. Zhao, X. Lin, X. Xu, *Nat. Commun.*, 4 (2013) 1.
44. ⁹ Kumagai, M. Sato, D. Tashima, *Electrochimem. Acta*, 114 (2013) 617.
45. M. R. Jisha, Y. J. Hwang, J. S. Shin, K. S. Nahm, T. P. Kumar, K. Karthikeyan, N. Dhanikaivelu, D. ⁴⁹ lpana, N. G. Renganathan, A. M. Stephan, *Material Chemistry and Physics*, 115 (2009) 33.
46. ³² Faraji, F. N. Ani, *Renew. Sust. Energ. Rev.*, 42 (2015) 823.
47. ¹⁸ Zhang, X. J. Li, J. F. Huang, W. Xing, Z. F. Yan, *Nanoscale Res. Lett.*, 11 (2016) 163.
48. H. Chen, Y-C. Guo, F. Wang, G. Wang, P-R.Qi, X-H. Guo, B. Dai, F. Yu, *New Carbon Materials*, 32 (2017) 592.
49. G. Zhang, Y. Chen, Y. Chen, H. Guo, *Materials Research Bulletin*, 102 (2018) 391.

Preparation of Activated Carbon Electrode from Pineapple Crown Waste as a Supercapacitor Application 131227

ORIGINALITY REPORT

25%

SIMILARITY INDEX

PRIMARY SOURCES

- 1

electrochemsci.org
Internet

134 words — 3%
- 2

aip.scitation.org
Internet

87 words — 2%
- 3

E. Taer, P. Dewi, Sugianto, R. Syech, R. Taslim, Salomo, Y. Susanti, A. Purnama, Apriwandi, Agustino, R. N. Setiadi. "The synthesis of carbon electrode supercapacitor from durian shell based on variations in the activation time", AIP Publishing, 2018
Crossref

61 words — 1%
- 4

Taer, Erman, Iwantono, Saidul Tua Manik, R. Taslim, D. Dahlan, and M. Deraman. "Preparation of Activated Carbon Monolith Electrodes from Sugarcane Bagasse by Physical and Physical-Chemical Activation Process for Supercapacitor Application", Advanced Materials Research, 2014.
Crossref

39 words — 1%
- 5

Erman Taer, Rika Taslim. "Brief review: Preparation techniques of biomass based activated carbon monolith electrode for supercapacitor applications", AIP Publishing, 2018
Crossref

38 words — 1%
- 6

Kim, Bo-Hye, Kap Seung Yang, and John P. Ferraris. "Highly conductive, mesoporous carbon nanofiber web as electrode material for high-performance supercapacitors", Electrochimica Acta, 2012.
Crossref

36 words — 1%

-
- 7 N S.M. Nor. "Supercapacitors using Binderless Activated Carbon Monoliths Electrodes consisting of a Graphite Additive and Pre-carbonized Biomass Fibers", International Journal of Electrochemical Science, 2017
Crossref 36 words — 1%
-
- 8 www.electrochemsci.org
Internet 34 words — 1%
-
- 9 Li, Q.. "In situ construction of potato starch based carbon nanofiber/activated carbon hybrid structure for high-performance electrical double layer capacitor", Journal of Power Sources, 20120601
Crossref 33 words — 1%
-
- 10 Mohammad A. Jafar Mazumder. "Synthesis and Evaluation of New Isoxazolidine Derivatives of Aldehyde as Corrosion Inhibitors for Mild Steel Corrosion in Acidic and Saline Media", International Journal of Electrochemical Science, 2016
Crossref 30 words — 1%
-
- 11 A. M. Donia. "Selective separation of Th(IV) from its solutions using amine modified silica gel produced from leached zircon", Journal of Radioanalytical and Nuclear Chemistry, 06/10/2011
Crossref 30 words — 1%
-
- 12 Guoxiong Zhang, Yuemei Chen, Yigang Chen, Haibo Guo. "Activated biomass carbon made from bamboo as electrode material for supercapacitors", Materials Research Bulletin, 2018
Crossref 29 words — 1%
-
- 13 d-nb.info
Internet 27 words — 1%
-
- 14 Razman, Nur Izzatie Hannah, Salasiah Endud, Zainab Ramli, Hendrik Oktendy Lintang, Izan Izwan Misonon, and Hanapi Mat. "Enhanced capacitance of a nitrogen-containing carbon-based nanocomposite via noncovalent functionalization method", Journal of Industrial and Engineering Chemistry, 2015. 26 words — 1%

-
- 15 scholarbank.nus.edu.sg 25 words — < 1%
Internet
-
- 16 Tokeer Ahmad, Irfan H. Lone, Mohd. Ubaidullah, Kelsey Coolhan. "Low-temperature synthesis, structural and magnetic properties of self-dopant $\text{LaMnO}_{3+\delta}$ nanoparticles from a metal-organic polymeric precursor", *Materials Research Bulletin*, 2013 25 words — < 1%
Crossref
-
- 17 Wang, Zicheng, Yan Wang, Xia Shu, Cuiping Yu, Jianfang Zhang, Jiewu Cui, Yongqiang Qin, Hongmei Zheng, Yong Zhang, and Yucheng Wu. "Hierarchical three-dimensional $\text{MnO}_2/\text{carbon}@ \text{TiO}_2$ nanotube arrays for high-performance supercapacitors", *RSC Advances*, 2016. 24 words — < 1%
Crossref
-
- 18 Feifei Wang, Xingbin Lv, Lili Zhang, Hualian Zhang, Yanfang Zhu, Zhufeng Hu, Yuxin Zhang, Junyi Ji, Wei Jiang. "Construction of vertically aligned PPy nanosheets networks anchored on MnCo_2O_4 nanobelts for high-performance asymmetric supercapacitor", *Journal of Power Sources*, 2018 23 words — < 1%
Crossref
-
- 19 R. Farma, M. Deraman, A. Awitdrus, I.A. Talib, E. Taer, N.H. Basri, J.G. Manjunatha, M.M. Ishak, B.N.M. Dollah, S.A. Hashmi. "Preparation of highly porous binderless activated carbon electrodes from fibres of oil palm empty fruit bunches for application in supercapacitors", *Bioresource Technology*, 2013 22 words — < 1%
Crossref
-
- 20 P.K. Johnston, E. Doyle, R.A. Orzel. "Acrylics: A Literature Review of Thermal Decomposition Products and Toxicity", *Journal of the American College of Toxicology*, 2016 20 words — < 1%
Crossref
-
- 21 Liang Liang, Minghua Zhou, Chaolin Tan, Xiaoyu Tian, Kerui Li. "Easily tunable hydrogel-derived 19 words — < 1%

heteroatom-doped hierarchically porous carbons as multifunctional materials for supercapacitors, CO₂ capture and dye removal", Microporous and Mesoporous Materials, 2018

Crossref

-
- | | | |
|-----------|---|-----------------|
| 22 | web.stanford.edu
<small>Internet</small> | 19 words — < 1% |
|-----------|---|-----------------|
-
- | | | |
|-----------|---|-----------------|
| 23 | digital.lib.washington.edu
<small>Internet</small> | 19 words — < 1% |
|-----------|---|-----------------|
-
- | | | |
|-----------|--|-----------------|
| 24 | Qingyong Wang. "Prussian-Blue-Doped Super-Activated Carbon as a High Performance Supercapacitor Electrode Material", International Journal of Electrochemical Science, 2016
<small>Crossref</small> | 18 words — < 1% |
|-----------|--|-----------------|
-
- | | | |
|-----------|---|-----------------|
| 25 | onlinelibrary.wiley.com
<small>Internet</small> | 18 words — < 1% |
|-----------|---|-----------------|
-
- | | | |
|-----------|---|-----------------|
| 26 | pubs.acs.org
<small>Internet</small> | 16 words — < 1% |
|-----------|---|-----------------|
-
- | | | |
|-----------|---|-----------------|
| 27 | www.degruyter.com
<small>Internet</small> | 16 words — < 1% |
|-----------|---|-----------------|
-
- | | | |
|-----------|--|-----------------|
| 28 | Hongyun Ma, Chun Li, Miao Zhang, Jong-Dal Hong, Gaoquan Shi. "Graphene oxide induced hydrothermal carbonization of egg proteins for high-performance supercapacitors", Journal of Materials Chemistry A, 2017
<small>Crossref</small> | 16 words — < 1% |
|-----------|--|-----------------|
-
- | | | |
|-----------|--|-----------------|
| 29 | Jiao Chen, Jianhui Qiu, Bin Wang, Huixia Feng, Kazushi Ito, Eiichi Sakai. "Fe₃O₄/biocarbon composites with superior performance in supercapacitors", Journal of Electroanalytical Chemistry, 2017
<small>Crossref</small> | 16 words — < 1% |
|-----------|--|-----------------|
-
- | | | |
|-----------|--|-----------------|
| 30 | Junayet Hossain Khan, Freddy Marpaung, Christine Young, Jianjian Lin et al. "Jute-derived microporous/mesoporous carbon with ultra-high surface area using a chemical activation process", Microporous and | 15 words — < 1% |
|-----------|--|-----------------|

-
- | | | |
|----|---|-----------------|
| 31 | diva-portal.org
<small>Internet</small> | 15 words — < 1% |
|----|---|-----------------|
-
- | | | |
|----|---|-----------------|
| 32 | Kolathodi, M. S., L. David, M. A. Abass, and G. Singh. "Polysiloxane-functionalized graphene oxide paper: pyrolysis and performance as a Li-ion battery and supercapacitor electrode", RSC Advances, 2016.
<small>Crossref</small> | 14 words — < 1% |
|----|---|-----------------|
-
- | | | |
|----|---|-----------------|
| 33 | oatao.univ-toulouse.fr
<small>Internet</small> | 14 words — < 1% |
|----|---|-----------------|
-
- | | | |
|----|---|-----------------|
| 34 | E. Taer, Apriwandi, Yusriwandi, W. S. Mustika, Zulkifli, R. Taslim, Sugianto, B. Kurniasih, Agustino, P. Dewi. "Comparative study of CO ₂ and H ₂ O activation in the synthesis of carbon electrode for supercapacitors", AIP Publishing, 2018
<small>Crossref</small> | 13 words — < 1% |
|----|---|-----------------|
-
- | | | |
|----|--|-----------------|
| 35 | Lim, Eunho, Haegyeom Kim, Changshin Jo et al. "Advanced Hybrid Supercapacitor Based on a Mesoporous Niobium Pentoxide/Carbon as High-Performance Anode", ACS Nano
<small>Crossref</small> | 13 words — < 1% |
|----|--|-----------------|
-
- | | | |
|----|---|-----------------|
| 36 | Mahendra Singh Yadav, Narendra Singh, Anuj Kumar. "Synthesis and characterization of zinc oxide nanoparticles and activated charcoal based nanocomposite for supercapacitor electrode application", Journal of Materials Science: Materials in Electronics, 2018
<small>Crossref</small> | 13 words — < 1% |
|----|---|-----------------|
-
- | | | |
|----|--|-----------------|
| 37 | Yan, Jun, Qian Wang, Tong Wei, and Zhuangjun Fan. "Recent Advances in Design and Fabrication of Electrochemical Supercapacitors with High Energy Densities", Advanced Energy Materials, 2013.
<small>Crossref</small> | 13 words — < 1% |
|----|--|-----------------|
-
- | | | |
|----|---|-----------------|
| 38 | www.chem.eng.psu.ac.th
<small>Internet</small> | 12 words — < 1% |
|----|---|-----------------|

39 Asroful Abidin, Chandra Wahyu Purnomo, Rochim Bakti Cahyono. "Hydro-char production from press-mud wastes of the sugarcane industry by hydrothermal treatment with natural zeolite addition", AIP Publishing, 2018

Crossref

12 words — < 1%

40 Demiral, İlknur, Canan Aydın Şamdan, and Hakan Demiral. "Production and characterization of activated carbons from pumpkin seed shell by chemical activation with ZnCl₂", Desalination and Water Treatment, 2016.

Crossref

12 words — < 1%

41 Junwei Lang, Xu Zhang, Bao Liu, Rutao Wang, Jiangtao Chen, Xingbin Yan. "The roles of graphene in advanced Li-ion hybrid supercapacitors", Journal of Energy Chemistry, 2018

Crossref

11 words — < 1%

42 ir.canterbury.ac.nz

Internet

11 words — < 1%

43 Xuan Du. "Studies on the performances of silica aerogel electrodes for the application of supercapacitor", Ionics, 01/27/2009

Crossref

11 words — < 1%

44 Changchao Dai, Jiafeng Wan, Yang Juan, Shanshan Qu, Tieyu Jin, Fangwei Ma, Jinqiu Shao. "H₃PO₄ solution hydrothermal carbonization combined with KOH activation to prepare Argemone wormwood-based porous carbon for high-performance supercapacitors", Applied Surface Science, 2018

Crossref

11 words — < 1%

45 zh.scientific.net

Internet

11 words — < 1%

46 old.kps.or.kr

Internet

10 words — < 1%

47 Yunpu Zhai. "Carbon Materials for Chemical

10 words — < 1%

- 48 Talam Kibona Enock, Cecil K. King'ondur, Alexander Pogrebnoi, Yusufu Abeid Chande Jande. "Biogas-slurry derived mesoporous carbon for supercapacitor applications", Materials Today Energy, 2017

10 words — < 1%

Crossref

- 49 Rifat Farzana, Ravindra Rajarao, Badekai Ramachandra Bhat, Veena Sahajwalla. "Performance of an activated carbon supercapacitor electrode synthesised from waste Compact Discs (CDs)", Journal of Industrial and Engineering Chemistry, 2018

9 words — < 1%

Crossref

- 50 Suchada Sirisomboonchai, Suwadee Kongparakul, Khanin Nueangnoraj, Haibo Zhang et al. "Enhanced electrochemical performances with a copper/xylose-based carbon composite electrode", Applied Surface Science, 2018

9 words — < 1%

Crossref

- 51 Foo, K.Y.. "Textural porosity, surface chemistry and adsorptive properties of durian shell derived activated carbon prepared by microwave assisted NaOH activation", Chemical Engineering Journal, 20120401

9 words — < 1%

Crossref

- 52 Bello, Abdulhakeem, Ncholu Manyala, Farshad Barzegar, Abubakar A. Khaleed, Damilola Y. Momodu, and Julien K. Dangbegnon. "Renewable pine cone biomass derived carbon materials for supercapacitor application", RSC Advances, 2016.

9 words — < 1%

Crossref

- 53 Mieczyslaw Scendo. "Metavanadate(V) Anions as Corrosion Inhibitor for Carbon Steel in Acid Chloride Solution", International Journal of Electrochemical Science, 2016

9 words — < 1%

Crossref

- 54 ices2016conference.com

9 words — < 1%

Internet

55	ccsenet.org Internet	9 words — < 1%
56	jmrt.com.br Internet	9 words — < 1%
57	L. Zheng, W. B. Li, J. L. Chen. " Nitrogen doped hierarchical activated carbons derived from polyacrylonitrile fibers for CO adsorption and supercapacitor electrodes ", RSC Advances, 2018 Crossref	8 words — < 1%
58	Damian Pérez-Quintanilla. "A New Generation of Anticancer Drugs: Mesoporous Materials Modified with Titanocene Complexes", Chemistry - A European Journal, 04/15/2009 Crossref	8 words — < 1%
59	Rangabhashiyam. S, Balasubramanian. P. "The potential of lignocellulosic biomass precursors for biochar production: Performance, mechanism and wastewater application—A review", Industrial Crops and Products, 2019 Crossref	8 words — < 1%
60	pubs.rsc.org Internet	8 words — < 1%
61	Xuan Du, Wei Zhao, Yi Wang, Chengyang Wang, Mingming Chen, Tao Qi, Chao Hua, Mingguo Ma. "Preparation of activated carbon hollow fibers from ramie at low temperature for electric double-layer capacitor applications", Bioresource Technology, 2013 Crossref	7 words — < 1%
62	Zheng Chang. "Study of the Enzyme-Free Glucose Biosensor Based on Ni ²⁺ @ Poly (Neutral Red) Hybrid Nanocomposites (Ni ²⁺ @PNR HN)/MWCNTs/Nafion Modified Electrode", International Journal of Electrochemical Science, 2018 Crossref	6 words — < 1%

Reda A. Ammar. "Synthesis, Coordination behavior, pH-titration

63 and Antimicrobial Activity Studies of Ternary Co(II) Complexes of Girard T and Glycine Oligopeptides", International Journal of Electrochemical Science, 2018 6 words — < 1%
Crossref

64 Qingfeng Yang, Yue Wang, Jing Wang, Fangbing Liu, Na Hu, Hanna Pei, Weixia Yang, Zhonghong Li, Yourui Suo, Jianlong Wang. "High effective adsorption/removal of illegal food dyes from contaminated aqueous solution by Zr-MOFs (UiO-67)", Food Chemistry, 2018 6 words — < 1%
Crossref

EXCLUDE QUOTES OFF
EXCLUDE BIBLIOGRAPHY OFF

EXCLUDE MATCHES OFF